Towards a Unified Approach for the Analysis of Failure Modes in FRP-Retrofitted Concrete Beams

A. Carpinteri, P. Cornetti, G. Lacidogna* and M. Paggi

Politecnico di Torino, Department of Structural Engineering and Geotechnics, Corso Duca degli Abruzzi 24, 10129, Torino, Italy

Abstract: The application of the external reinforcement makes rather complex the scenario of the possible failure modes in reinforced concrete beams retrofitted with FRP. The far more commonly observed failure modes are: (i) edge debonding of the FRP sheet, (ii) intermediate crack induced debonding and (iii) beam failure due to diagonal (shear) crack propagation. In the present study we revisited the competition between all the possible failure modes that can occur in this structural element. To this aim, different analytical models based on linear and non-linear fracture mechanics are developed and harmonized. As a result, useful failure maps are analytically determined, giving, for each failure mode, the critical load of activation as a function of the main parameters governing the problem, i.e. the mechanical properties of the constituent materials, the amount of reinforcement and its bonding length, as well as the size and slenderness of the structural element. The studies presented in this paper are mainly intended to establish guidelines for the future development of these concepts towards a unified mathematical approach. Indeed, once the validity of this unified approach is confirmed, also by comparison with further experimental data, it will be possible to remove some of the simplifying assumptions we used in this analysis to reach a more comprehensive analytical formulation.

Key words: edge debonding, intermediate crack induced debonding, shear failure, multi-layered beam theory, asymptotic analysis.

1. INTRODUCTION

Structural rehabilitation is required whenever design mistakes, executive defects or unexpected loading conditions are assessed. In these cases, the use of a strengthening technique may be required in order either to increase the load carrying capacity of the structure, or to reduce its deformations. The problems related to upgrading, maintenance and structural rehabilitation of civil structures have a strong economic and social impact. For instance, the European Union has estimated in approximately 84,000 the number of reinforced and prestressed concrete bridges requiring maintenance and structural strengthening in the next few years, with an estimated annual budget of 318 MEuro. In this context, the use of a strengthening method based on high performance composites turns out to be more convenient than traditional techniques. This is specially true if the economic evaluation takes into account the duration of the intervention, the necessary equipments, the costs related to the possible out-of-order period of the structure, as well as the expected lifetime of the strengthened structure itself.

The choice of the proper rehabilitation technique and the assessment of its performance and durability clearly represent outstanding research points. Among the different rehabilitation strategies, bonding of FRP (Fiber Reinforced Polymers) sheets is becoming increasingly popular with reinforced concrete members (Hollaway and Leeming 1999; Oehlers and Seracino 2004). The growing interest of the scientific community in these

* Corresponding author. Email address: giuseppe.lacidogna@polito.it; Fax: +39-011-5644-899; Tel: +39-011-5644-871.

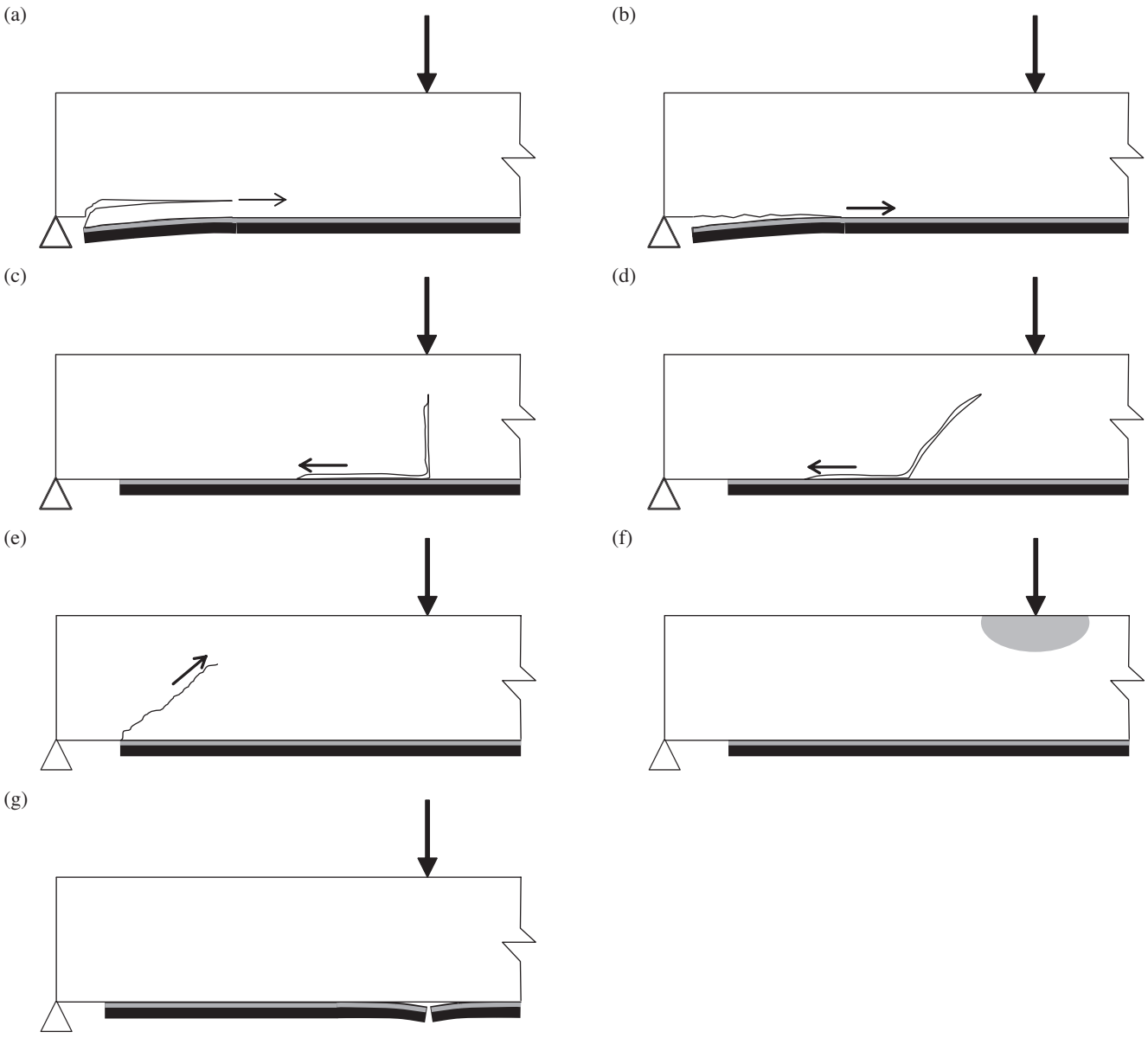

Figure 1. Failure mechanisms for three point bending concrete beams strengthened by FRP strips: (a) concrete cover separation (for RC beams); (b) edge FRP debonding; (c) intermediate flexural crack induced debonding; (d) intermediate flexural-shear crack induced debonding; (e) diagonal shear crack failure; (f) concrete crushing; (g) bending failure (FRP rupture). Thin arrows represent direction of crack propagation (when a crack is present)

advanced strengthening techniques is also testified by the recent publication of new guidelines and standards for the rehabilitation of reinforced concrete structures (ACI 440R 1996; fib Bulletin 2001; JCI 2003).

On the other hand, the application of the external reinforcement makes the scenario of the possible failure modes in reinforced structural elements rather complex. For instance, focusing our attention on reinforced concrete beams in bending retrofitted with FRP, we should mention the following main failure modes:

- Edge debonding of the FRP sheet, Figures 1(a,b) (David *et al*. 1993; Leung 2001, 2004; Leung and Yang 2006; Carpinteri *et al*. 2007a, b);
- Intermediate crack induced debonding, Figures 1(c,d) (Alaee and Karihaloo 2003; Teng *et al*. 2003; Leung 2004; Wang 2006; Cornetti *et al*. 2007);
- Beam failure due to diagonal (shear) crack propagation, Figure 1(e) (Ahmed *et al*. 2001, Carpinteri *et al*. 2007c);
- Beam failure due to concrete crushing at the extradox, Figure 1(f) (Arduini *et al*. 1997);
- Beam failure in bending, Figure 1(g) (Arduini et al. 1997).

Among them, edge debonding of the FRP, intermediate crack induced debonding and shear failure have been far more commonly revealed in experimental tests (see Figure 2). As regards edge debonding of FRP and shear failure, damage initiates near the FRP cut-off points due to the presence of a stress concentration or even a stress intensification caused by the elastic mismatch between FRP and concrete. As a consequence, either a pure FRP delamination or a diagonal crack growth can occur. Moreover, in the latter case, depending on the amount of steel reinforcement and thickness of the concrete cover, the diagonal crack may also give rise to concrete cover separation. In any case, this failure mode should be carefully distinguished from the pure FRP delamination and should be interpreted in the same framework as that for shear failure, since it occurs far away from the FRP-concrete interface. We have also to remark that edge debonding and shear crack propagation are strongly in competition between each other and such a competition is ruled by the mechanical properties of the constituent materials (concrete, fibers, adhesive), by the presence of steel bars, as well as by the slenderness and the size of the structural element.

To make the scenario even more complex, it is also possible to experimentally observe different directions of delamination (Teng *et al*. 2003). The delamination of the FRP sheet can in fact take place both from the beam

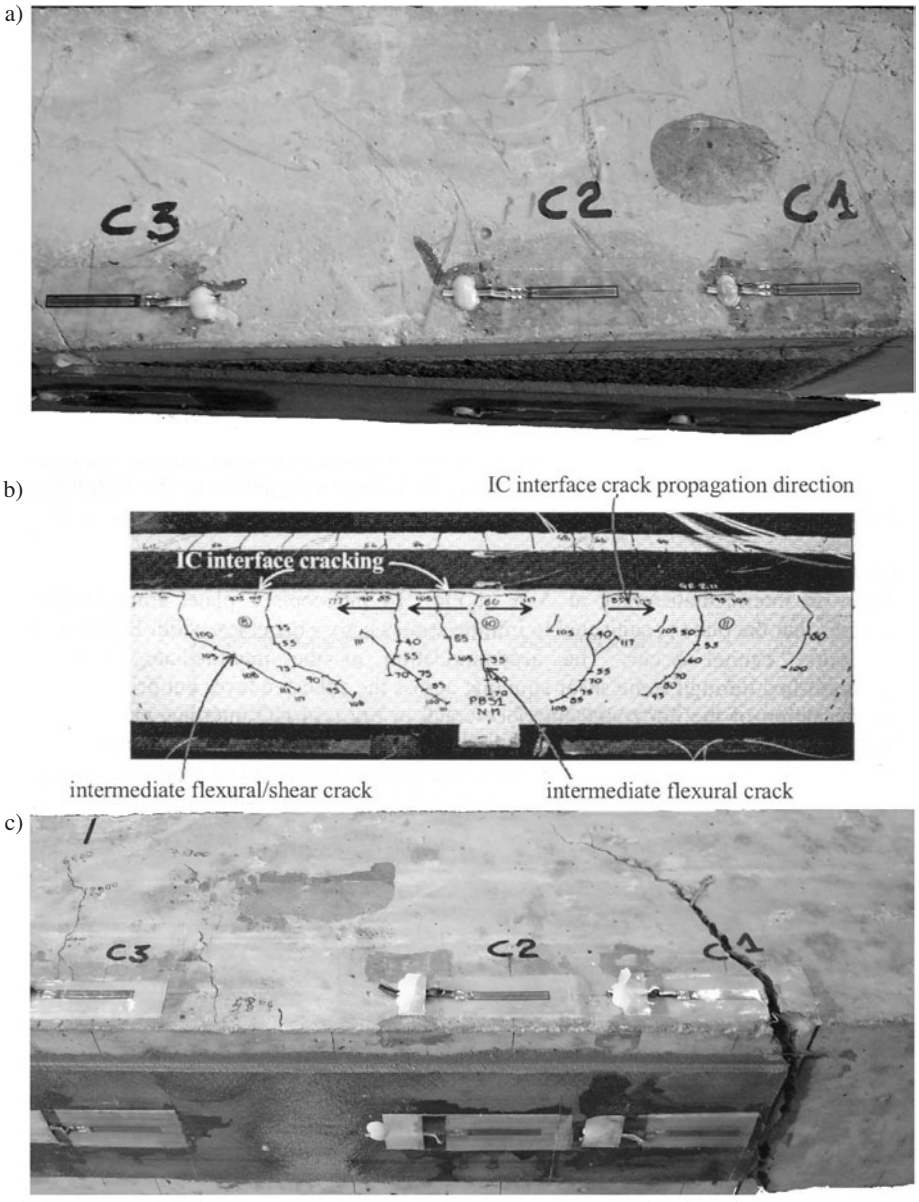

Figure 2. Failure mechanisms for three point bending concrete beams strengthened by FRP strips: (a) edge FRP debonding; (b) intermediate flexural crack induced debonding (Oehlers and Seracino 2004); (c) diagonal shear crack failure

supports towards the mid-span position, or in the opposite direction, i.e., from the mid-span position towards the supports. While in the first instance delamination is due to the stress concentration originated by the variation of the resistant cross-section, in the second case delamination takes place in correspondence of flexural cracks developed in the tensile zone of the concrete beam. Such cracks would be stable, but they give rise to stress concentrations at the interface between FRP and concrete. Under certain critical conditions, these stress concentrations can finally lead to FRP delamination. This failure mode, referred to as IC debonding, is perhaps the most complex to analyze, since the FRP delamination is related to flexural cracks that are not present in the original beam geometry and that are developed during the loading process.

The failure modes related to FRP delamination have been extensively investigated in the literature. The reasons are essentially two: on the one side, in fact, this failure mode is a novelty, in the sense that it is characteristic of retrofitted beams; on the other side, these failure modes are brittle, being the crack propagation between FRP and concrete highly unstable (Carpinteri *et al*. 2007b): it is therefore a particularly dangerous phenomenon that we have to carefully consider for a safe structural design. As regards the mathematical models available in the literature, most of them focus on the problem of edge debonding in steel plated and FRP strengthened beams (Smith and Teng 2002a,b). Shearing and peeling stresses in the adhesive layer of a beam with a strengthening plate bonded to its soffit were determined in (Taljsten 1997; Malek *et al*. 1998; Ascione and Feo 2000; Smith and Teng 2001). The analysis of interface tangential and normal stresses in FRP retrofitted RC beams was also recently re-examined in (Rabinovitch and Frostig 2001; Rabinovitch 2004), along with a fracture mechanics model for the prediction of edge delamination. The problem of IC debonding has also been modelled according to a bridged crack formulation (Leung 2001; Alaee and Karihaloo 2003).

The aim of the present paper is to propose a novel unified approach for the analysis of the competition between the aforementioned failure modes typical of reinforced concrete beams retrofitted with FRP. From the state-of-the-art survey, it is clear that the complexity of the scenario will demand the development and harmonization of several analytical and numerical models based on the concepts of linear and non-linear fracture mechanics. As an example, the propagation of flexural and shear cracks in reinforced concrete beams can accurately be analyzed according to the bridged-crack model, which permits to take into account the effect of bridging exerted by the steel bars and the FRP sheet on the crack pattern. At the same time, it will be shown that the phenomena of edge and IC debonding and their interaction can be analytically modelled according to the theory of layered beams with shear deformable interfaces. A more accurate description of edge delamination can also be achieved by using the cohesive crack model in the finite element framework, which permits to take into account the effect of both shearing and peeling stresses at the FRP-concrete interface. Finally, it will be shown that the problem of shear crack propagation can be described according to an asymptotic analysis of stress-singularities due to bonding of dissimilar materials (see also Bogy 1971; Carpinteri and Paggi 2005, 2007 for mathematical details). This approach will permit to address the problem of competition between shear crack growth and edge delamination and to highlight the related size-scale effects (see also the experimental work by Maalej and Leong 2005, which represents the first attempt to address this complex problem). It is worth noting that the proposed models permit not only to determine the critical loads for the onset of each failure mode, but also to study the fundamental issue of stability of the crack propagation. Moreover, the studies presented in this paper are mainly intended to establish guidelines for the analysis of FRP retrofitted RC beams towards an integrated mathematical approach. Indeed, once the validity of this unified approach is confirmed, for example by comparison with further experimental data, it will be possible to remove some of the simplifying assumptions we used in this analysis to reach a more comprehensive analytical formulation.

2. FRP DEBONDING

It has been already observed that most of the researchers have focused their attention on the debonding failure mechanism, partly because it is typical of strengthened structures, partly because it is a catastrophic failure. In fact, the propagation of the interfacial crack is usually unstable: it is therefore of the maximum importance for the designer to avoid the possible rising of FRP debonding, since, in such a case, the structural behaviour is highly brittle.

The analysis of the phenomenon is rather complex even because different debonding mechanisms can take place. The delamination of the FRP may occur either toward the mid-span or toward the supports (Figures 1(a,b,c,d)). While in the former case, named edge debonding, the cause of the debonding is represented by the stress concentration due to the change in the resistant cross section, in the latter case the stress concentration

occurs in correspondence with flexural cracks in the tensile side of the concrete beam. Such cracks usually appear as the load increases and then stop when they reach a certain depth; nevertheless, they may cause the delamination of the FRP sheet from the crack mouth toward the edges. This is the reason why such a failure mode is sometimes referred to as intermediate crack induced debonding or, simply, IC debonding.

It is worth observing that IC debonding is even harder to describe with respect to edge debonding, essentially because the flexural crack are not present in the original (i.e. undamaged) geometry but they appear during the loading process. Furthermore, the debonding can start either from the mid-span or from an intermediate point: in the first case, we refer to the failure mode as intermediate flexural crack induced debonding or, more simply, to central debonding; otherwise the mechanism is named intermediate shear-flexural crack induced debonding (Teng *et al*. 2003).

In order to predict the critical load at which the edge debonding phenomenon takes place, several models have been proposed to evaluate the interfacial stresses. They focus onto the prediction of the stresses in the vicinity of the edge of the FRP strip. These stresses are then used to predict the peak load. A critical review of these models can be found in the papers by Muckopadhyaya and Swamy (2001) and Smith and Teng (2001).

However, because of the brittleness of the debonding process, an energy approach seems to be more effective, since stress-based failure criteria are more suitable for gradual and ductile failures. An energy-based fracture criterion has recently been proposed by Rabinovitch (2004) by applying the linear elastic fracture mechanics (LEFM) concept of energy release rate to a class of mechanical models, from equivalent beam theory to a full 2D elastic medium solution. However no easy analytical expressions for the debonding load have been provided because of the complexity of the energy approach to the problem under examination. On the other hand, it has been proved (Cornetti *et al*. 2007) that, if the adhesive layer is represented by a bed of horizontal springs, i.e. it acts as a shear lag, a simple relationship between the maximum shear stress τ_{max} and the energy release rate $\mathcal{G}$ holds:

$$\mathcal{G} = \frac{\tau_{max}^2}{2G_a} h_a \tag{1}$$

where G_a and h_a are respectively the shear modulus and the thickness of the adhesive layer. By means of Eqn 1, the application of the LEFM criterion $\mathcal{G} = \mathcal{G}_c$ is straightforward. It is worth observing that Eqn 1 is somehow analogous the well-known Irwin's relationship between the strain energy release rate and the stress-intensity factor: $\mathcal{G} = K_I^2/E$. They both relates an energy parameter, i.e. the strain energy release rate, to a stress field parameter through an elastic modulus. The difference lies in the stress intensification for the crack in an homogeneous medium and the stress concentration provided by the shear lag model.

Eqn 1 can be easily generalized in order to take into account also the peeling stresses, assumed to be constant across the adhesive thickness. Nevertheless, the authors, in order to have a global insight into the problem, prefer to start from a model as simple as possible, so that it can be handled analytically. For this reason we assumed that (i) the adhesive layer acts as a shear lag and (ii) the interface shows a brittle behaviour so that LEFM can be applied. Although these hypotheses may appear rather strong, it is worth observing that, in the computations performed by Rabinovitch (2004), the peeling stresses seem to affect slightly the strain energy release rate; furthermore the generalization of Eqn 1 to softening interfaces should be achievable, as showed recently by Leung and Yang (2006) in the case of a rigid substrate.

Based on the previous hypotheses, the determination of the critical load causing FRP debonding for a three point bending beam (Figure 3) can be reduced to the determination of the strain inside the FRP strip ε_r, since the shear stress in the adhesive is provided by its first derivative. The governing equation (Carpinteri *et al*. 2007a) in dimensionless form reads:

$$\frac{d^2\varepsilon_r}{d\zeta^2} - \beta^2\varepsilon_r = f(\zeta), \qquad 0 \le \zeta \le \zeta_r \tag{2a}$$

$$\beta^2 = \frac{G_a l^2}{4E_r h_r h_a}(1+4\rho) \tag{2b}$$

where ζ is the longitudinal coordinate normalized to half of the beam span, i.e. $\zeta = 0$, $\zeta = \zeta_r$, $\zeta = 1$ correspond to points located, respectively, at the mid-span, at the FRP edge ($0 < \zeta_r < 1$) and at the support; $f(\zeta)$ is a function proportional to the bending moment. The dimensionless parameter β^2 depends on material and geometrical properties (see Figure 3): l is the beam span; E_r and h_r are respectively the Young's modulus and the thickness of the FRP plate; ρ is the fraction of the mechanical reinforcement, defined as the ratio between the area of the FRP and that of the beam cross section times the ratio between the respective elastic moduli.

2.1. Edge vs. IC Debonding

In order to have a preliminary insight into the competition between the edge debonding and flexural crack induced FRP debonding, we may assume that the flexural crack has fully developed before the debonding

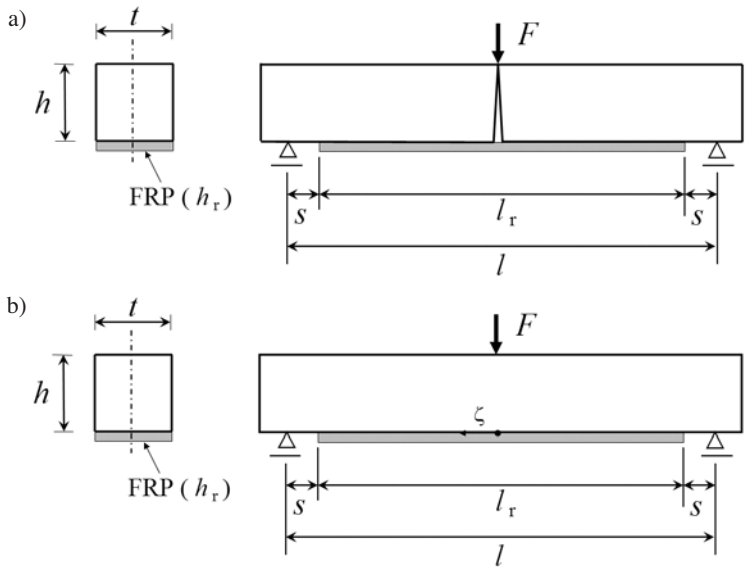

Figure 3. Scheme of the three-point bending test: notched beam or beam with a fully developed flexural crack (a); unnotched beam (b)

crack starts propagating along the interface (Figure 3(a)). Note that this geometry is the one actually used in some laboratory tests (Accardi 2004). In such a case, the strain in the FRP strip at mid-span $\bar{\varepsilon}_r$ is known from equilibrium considerations and the boundary conditions reads therefore:

$$\varepsilon_r = 0, \quad \text{if} \quad \zeta = \zeta_r \tag{3a}$$

$$\varepsilon_r = \bar{\varepsilon}_r, \quad \text{if} \quad \zeta = 0 \tag{3b}$$

If no flexural crack is present (Figure 3(b)), i.e. no damage has occurred, the boundary condition (3b) at mid-span is replaced by the symmetry condition:

$$\frac{d\varepsilon_r}{d\zeta} = 0, \quad \text{if} \quad \zeta = 0 \tag{4}$$

From a mathematical point of view, the boundary conditions (3) give rise to two boundary layers at the extremities of the domain of integration. Physically, these boundary layers correspond to a shear stress concentration at the FRP edge and at the mouth of the flexural crack. The maximum values of the shear stress in the adhesive can hence be computed and, by means of Eqn 1, LEFM finally leads to the debonding failure loads. On the other hand, if the flexural crack is missing, the boundary condition (4) is to be used and only a boundary layer appears at the FRP ends, i.e. the shear stresses concentrate only at the edges. In such a case, only the edge debonding may occur.

An interesting aspect of the problem is the effect of the percentage of the mechanical reinforcement ρ. Increasing ρ, the critical load causing IC debonding increases whereas the load corresponding to edge debonding decreases. This is in agreement with experimental observations (Leung 2001), and shows that the model is able to catch the basic features of the debonding phenomena.

By comparing the strain energy release rates corresponding respectively to IC and edge debonding, it is finally possible to study the competition between the failure mechanisms. The result turns out to be quite simple: IC debonding prevails for relative reinforcement lengths higher than

$$\zeta_r = \frac{8\rho - 1}{6\rho} \tag{5}$$

otherwise, edge delamination occurs. Since $0 \le \zeta_r \le 1$, it is found that for $\rho \ge 0.125$ the central debonding will always take place; for $\rho \ge 0.5$ the edge debonding will always prevail. However, as the mechanical percentage of reinforcement ρ is typically closer to 0.125 (or even lower) than to 0.5, it can be stated that, for a cracked beam, the usual failure mode is the central debonding. This is perfectly in agreement with the experimental observations (Leung 2001). In other words, edge delamination will prevail only for very stiff or thick FRP sheets and for low reinforcement lengths. For the sake of clarity, Eqn 5 is plotted in Figure 4, where the regions corresponding to the different failure mechanisms are highlighted.

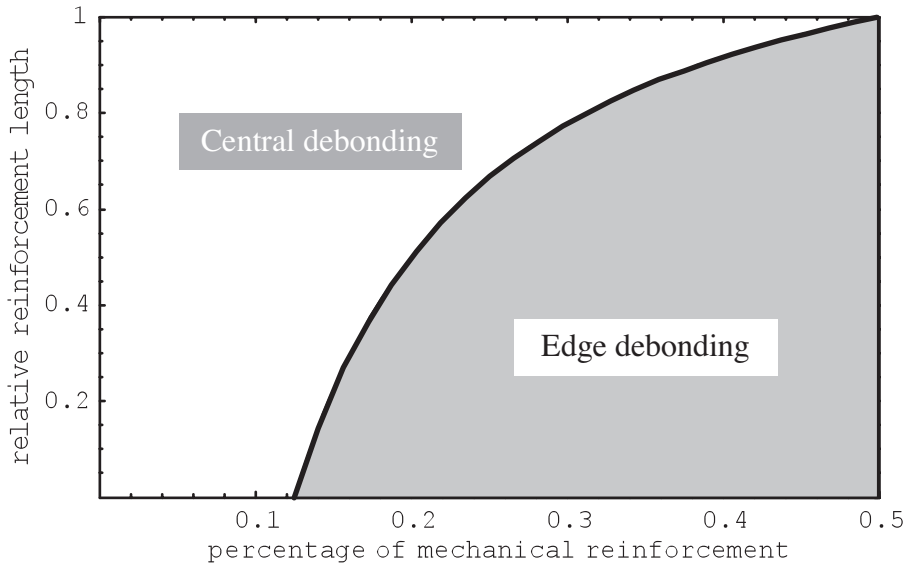

Figure 4. Failure mechanism as a function of geometrical and mechanical parameters

2.2. Flexural Crack Growth vs. IC Debonding

In order to study the competition between the flexural crack and the interfacial crack starting from mid-span (Figure 5), the bridged crack model (Carpinteri 1981, 1984) can be used (see, e.g., Leung 2001). The procedure for its application to FRP strengthened beams is briefly sketched below.

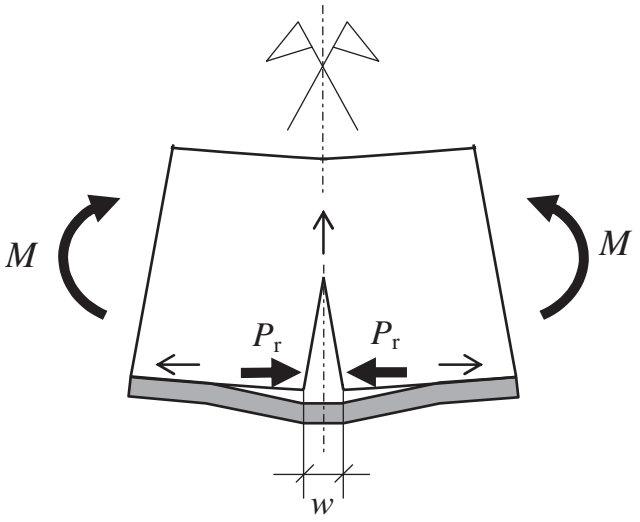

Figure 5. The bridged crack: the thick arrows represent respectively the bending moment and the closure actions exerted by the FRP strip on the flexural crack; the thin arrows represent the possible crack growth directions

The FRP sheet is modelled by means of the static action P_r it exerts on the faces of the cracked section of the beam. Then, one has to compute the opening w of the crack lips at the bottom of the beam (CMOD) as a function of the force in the FRP strip and of the bending moment M:

$$w = \lambda_{FM} M - \lambda_{FF} P_r \tag{6}$$

where λ_{FM} e λ_{FF} are the compliances referring to the bending moment and the FRP sheet action, respectively; details can be found in Carpinteri (1981, 1985).

The critical value M_F of the bending moment corresponding to the onset of flexural crack propagation can be obtained by equating the total stress-intensity factor to its critical value (fracture toughness of the beam material). The critical condition therefore reads:

$$K_{IC} = K_I(M) + K_I(P_r) \tag{7}$$

The bridged crack therefore provides a relationship between the CMOD and the applied load, as well as a criterion for propagation of the flexural crack inside the beam. However, in order to solve the problem, the relationship between the force P_r in the FRP sheet and the crack mouth opening displacement w is required. Coherently with the model outlined in the previous section, this goal can be achieved by a further application of the shear lag model (Stang *et al*. 1990). Symbolically:

$$P_r = P_r(w) \tag{8}$$

Finally, by means of LEFM, it is possible to find out the critical value P_r^* corresponding to the FRP delamination:

$$P_r = P_r^* \tag{9}$$

where P_r^* turns out to be a function of geometrical and mechanical properties as well as of the fracture energy of the interface.

The problem is now completely developed and the algorithm is as follows. For a given geometry, Eqns 6 and 8 allows to obtain the SIF at the flexural crack tip as well as the force in the FRP sheet. If, increasing the load, the critical condition (7) is reached before critical condition (9), it means that the flexural crack is growing (since $M = M_F$); otherwise, the interfacial crack starts propagating (since $P_r = P_r^*$). The geometry has therefore to be changed accordingly and the procedure is repeated up to final failure.

To summarize, by means of Eqns 6 to 9, the bridged crack model allows one to investigate the behaviour of the retrofitted beam when a shallow flexural crack is present and to evaluate the competition between the flexural crack propagation and the FRP central debonding. Preliminary results (Cornetti *et al*. 2007) show that flexural crack propagation usually precedes the onset of central debonding. The flexural crack propagates unstably at first; then it slows down stops in the upper, compressed part of the concrete beam. In this region the flexural crack propagation is stable, i.e. a load increment is needed to have a further crack advancement. Hence the load can reach the threshold value triggering the IC debonding failure, which, as it will be shown in Section 4, is unstable up to final collapse. This structural behaviour shows that IC debonding can be studied effectively with the model presented in the previous section, where the flexural crack is already fully developed. A complete parametrical analysis, as well as the analytical details on how to consider the beam deformation in the shear lag model coupled with the bridged crack, will appear elsewhere.

3. ASYMPTOTIC APPROACH TO SHEAR FAILURE AND EDGE DEBONDING

According to Linear Elastic Fracture Mechanics, the FRP cut-off point can be a source of stress-singularities due to the mismatch in the elastic properties of concrete and FRP. The geometry of a plane elastostatic problem consisting of two dissimilar isotropic, homogeneous wedges of angles equal to $\gamma_1 = \pi$ and $\gamma_2 = \pi/2$ perfectly bonded along their interface is schematically shown in Figure 6.

In this general case, the singular components of the stress field can be written as follows:

$$\sigma_{ij} = K^* r^{(\mathrm{Re}\,\lambda - 1)} S_{ij}(\theta) \tag{10}$$

where K^* is referred to as generalized stress-intensity factor (Carpinteri 1987). The parameter λ defines the order of the stress-singularity and can be obtained according to an asymptotic analysis of the stress field (Williams 1952; Bogy 1971; Carpinteri and Paggi 2005, 2007). According to this approach, the parameter λ is determined by solving a nonlinear eigenvalue problem resulting from the imposition of the boundary conditions. In the present problem, they consist in the stress-free boundary conditions along the free edges, and in the continuity conditions of stresses and displacements along the bi-material interface. This fully bonded bi-material interface would represent the typical condition observed under moderate applied external loads before the appearance of any damage.

Since we are interested in the analysis of the singular terms of the stress field, we are concerned only with those values of λ which may lead to singularities. This fact, along with the condition of continuity of the displacement field at the vertex where regions meet, imply that we are seeking for eigenvalues in the range $0 < \mathrm{Re}\,\lambda < 1$.

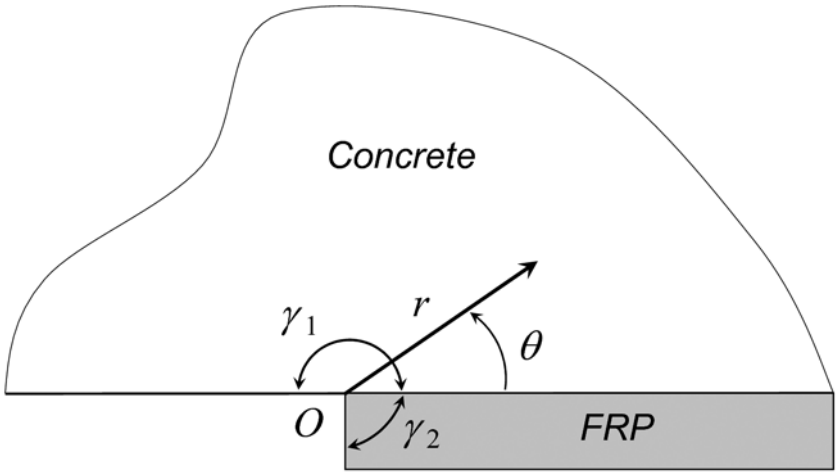

Figure 6. Scheme of the bi-material wedge composed of concrete and FRP

Function $S_{ij}(\theta)$ in Eqn 10 is the eigenfunction of the problem and it locally describes the angular variation of the stress field near the singular point, O. It has to be remarked that, since both λ and $S_{ij}(\theta)$ are determined according to the asymptotic analysis, they solely depend on the boundary conditions imposed in proximity of the singular point.

Moreover, from dimensional analysis arguments (Carpinteri 1987), it is possible to consider the following expression for the generalized stress-intensity factor:

$$K^* = \frac{Fl}{th^{1+\mathrm{Re}\,\lambda}} f\left(\frac{l}{h}, \zeta_r, \rho\right) \tag{11}$$

where function f depends on the boundary conditions far from the singular point and can be determined according to a FE analysis taking into account the actual geometry of the tested specimen and the boundary conditions. For the sake of generality, this function depends on the slenderness of the tested beams through the ratio l/h, on the relative length of the FRP sheet as compared to the beam span, ζ_r, and on the mechanical percentage of external reinforcement, ρ, which takes into account both the relative thickness of the FRP sheet as compared to the beam depth and the modular ratio between FRP and concrete. In practical applications, the ratio l/h should range between 10 and 20, whereas ζ_r is usually comprised between 0.7 and 0.9. The mechanical percentage of the external reinforcement, ρ, can also have one order of magnitude of variation. In fact, if the modular ratio is approximately constant, $E_r/E_c \sim 10$, the FRP thickness can be varied by bonding together several laminae of FRP. If we consider a typical thickness of 1.4 mm for each lamina, and we vary the number of laminae from 1 to 4, the mechanical percentage varies from 0.02 to 0.32 in its turn for the typical beam depths used in civil engineering.

The functional dependence in Eqn 11 has also important consequences for the design of experiments. In fact, a complete description of the mechanical response through the realization of *failure maps* can only be gained if all the nondimensional parameters entering Eqn 11 are varied.

The critical load corresponding to the onset of edge delamination can be determined by setting the generalized stress-intensity factor equal to the critical stress-intensity factor for the interface. This approach, well-established for the analysis of bonded joints (Reedy and Guess 1993; Qian and Akisanya 1999; Carpinteri and Paggi 2006), yields the following equation:

$$F_C^{\mathrm{deb}} = K_{C,\mathrm{int}}^* \frac{th^{1+\mathrm{Re}\,\lambda}}{l} \frac{1}{f} \tag{12}$$

An analogous reasoning can be proposed for the analysis of the onset of shear failure, i.e. before the development of the crack-bridging effect due to steel reinforcement. In this case, we can postulate the existence of a small vertical crack in concrete at the FRP cut-off point simulating an initial defect. This crack may result in a sudden diagonal propagation leading to premature failure of the beam.

The stress field at the crack tip is again singular, but with the order of the singularity typical of a crack inside a homogeneous material (Carpinteri 1987; Bocca *et al*. 1990):

$$\sigma_{ij} = Kr^{-1/2} F_{ij}(\theta) \tag{13}$$

where function $F_{ij}(\theta)$ locally describes the angular variation of the stress field near the crack tip. From dimensional analysis considerations, it is possible to write the following expression for the Mode I stress-intensity factor:

$$K_{\mathrm{I}} = \frac{Fl}{th^{3/2}} g\left(\frac{a_0}{h}, \frac{l}{h}, \zeta_r, \rho\right) \tag{14}$$

where function g depends again on the boundary conditions far from the singular point and can be determined according to a FE analysis on the actual geometry of the tested specimen. The additional parameter a_0 with respect to edge debonding denotes the initial crack length.

Crack propagation in this case takes place under mixed mode, although the Mode I stress-intensity factor is numerically prevailing. Under such assumptions, the critical load corresponding to the onset of shear crack propagation is reached when the Mode I stress-intensity factor equals the critical value of concrete. This condition yields the following equation:

$$F_C^{\mathrm{shear}} = K_{\mathrm{IC}} \frac{th^{3/2}}{l} \frac{1}{g} \tag{15}$$

3.1. Shear Crack Propagation vs. Edge Debonding

For a given tested beam, i.e., for a given beam geometry and material combination, the ratio between the critical loads for the onset of edge debonding and for the onset of shear crack propagation into concrete can be written as:

$$\frac{F_C^{\mathrm{deb}}}{F_C^{\mathrm{shear}}} = \left(\frac{K_{C,\mathrm{int}}^*}{K_{\mathrm{IC}}} \frac{g}{f}\right) h^{(\mathrm{Re}\,\lambda - 1/2)} \tag{16}$$

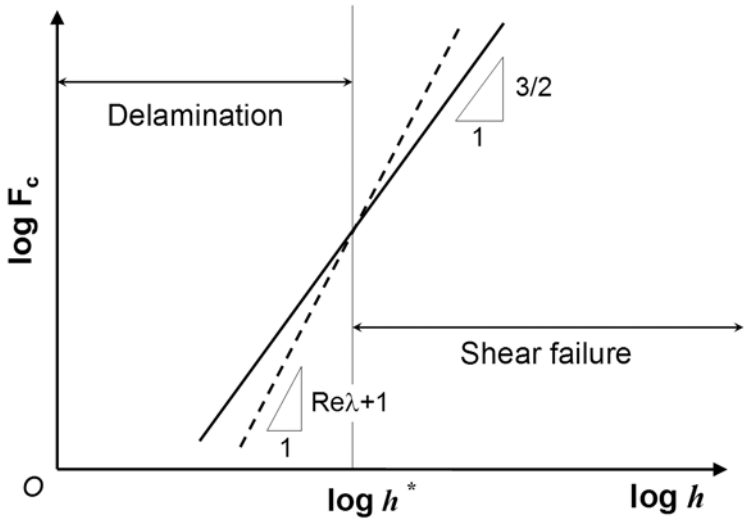

Figure 7. Edge debonding vs. shear failure: dashed line corresponds to edge debonding, solid line corresponds to shear failure

which is a nonlinear function of the beam depth. In addition, it is possible to recast Eqns 12 and 15 in a logarithmic form:

$$\log F_C^{\text{deb}} = \log\left(\frac{tK_{C,\text{int}}^*}{lf}\right) + (1+\text{Re}\,\lambda)\,\log h \qquad (17)$$

$$\log F_C^{\text{shear}} = \log\left(\frac{tK_{IC}}{lg}\right) + \frac{3}{2}\log h \qquad (18)$$

These equations are qualitatively plotted as functions of the beam depth in Figure 7. As expected, the higher the beam depth, for a beam slenderness *l*/*h*, the higher the critical load of failure. The intersection point between the two curves defines the critical beam size corresponding to the transition from pure edge debonding to shear failure. Moreover, since the real part of the eigenvalue λ is usually higher than 0.5, we expect a prevalence of shear failure in geometrically similar larger beams. In fact, if we consider E_r = 200 GPa and E_c = 30 MPa as the representative values of the Young's moduli of concrete and FRP, then the asymptotic analysis gives λ=0.58.

4. STABILITY OF THE DEBONDING PROCESSES

Within the framework outlined in Section 2, it is possible to achieve also the post-peak structural response, e.g. the load vs. mid-span deflection curves during debonding. As expected, both IC and edge debonding are characterized by an unstable interfacial crack propagation if the process is load-controlled (see Figures 8 and 10). This analytical finding confirms what was stated in the introduction, i.e. the failure due to FRP delamination is a catastrophic one and, hence, should be accurately avoided. However, varying to the delamination direction, the post-peak structural behaviour strongly changes.

For what concerns the edge debonding of the FRP strip, it is observed that, for usual values of material and geometric quantities, *snap-back instability* always occurs, i.e. there is a sudden drop in the load carrying capacity at the debonding initiation even if the process is displacement controlled (see Figure 8). This is due to the positive slope of the initial part of the softening branch. On the other hand, if the beam does not collapse because of other failure mechanisms, it can be seen that, increasing the mid-span displacement beyond the snap-back, the load starts growing again, the slope of the load vs. displacement curve being given now by the compliance of the unreinforced structure. As a consequence, if the process were load-controlled, a sudden (positive) jump in the mid-span deflection should appear. This phenomenon is named *snap-through instability*. For a detailed analysis and definitions of such instabilities in concrete structures, the reader is referred to the papers by Carpinteri (1985, 1989a,b).

More in details, the plot in Figure 8 refers to the following material and geometrical values (see also Figure 3(b)): the beam is characterized by a span length equal to 1 m, a depth equal to 0.12 m and a width equal to 0.10 m; the Young's moduli of concrete and FRP are respectively 30 GPa and 210 GPa, whereas the Poisson's ratio is 0.2 for both the materials; the FRP strip is 3 mm thick and the relative reinforcement length is 75%; the adhesive layer is 2 mm thick and the shear

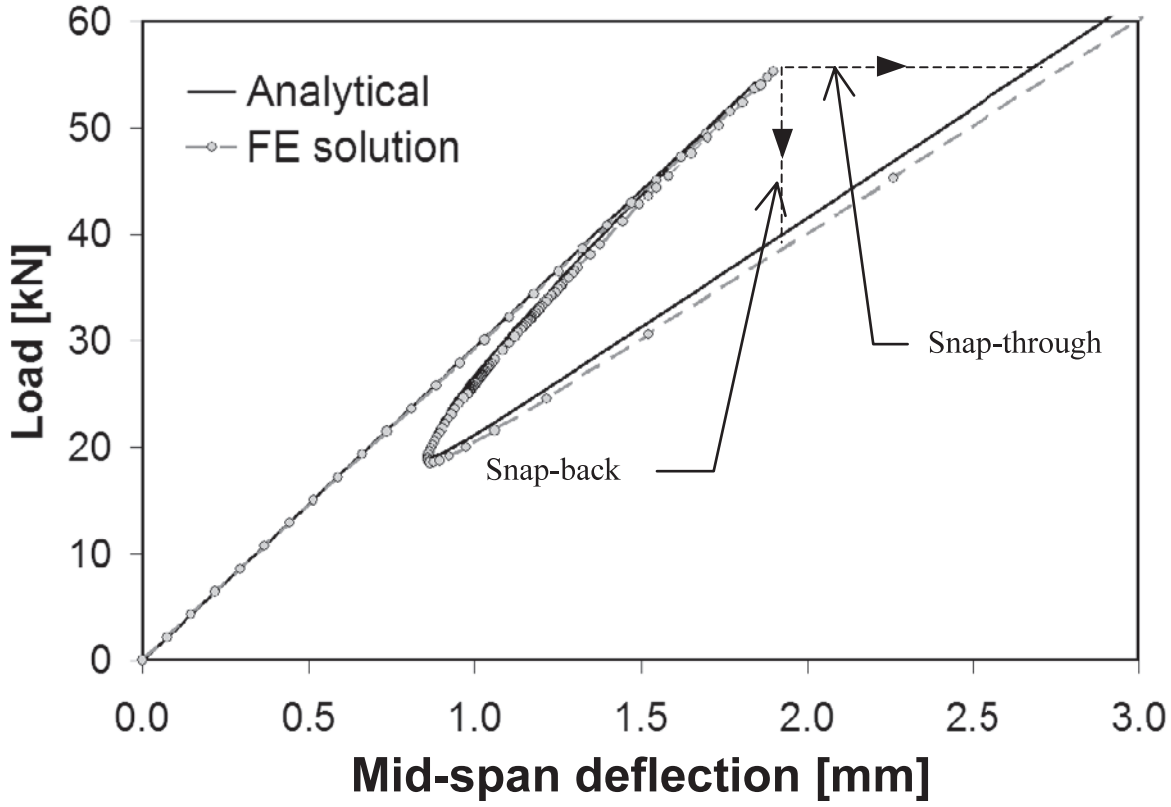

Figure 8. Load vs. mid-span deflection for a retrofitted concrete beam undergoing to FRP edge delamination: the solid line indicates the analytical prediction obtained according to the shear-lag model, whereas the dashed line corresponds to the FE solution

modulus is 720 MPa; finally, the parameter governing the debonding process, i.e. the Mode II fracture energy, is taken equal to 65 N/m.

In order to check the validity of the shear lag model outlined in Section 2, a comparison with a numerical analysis using the commercial finite element code LUSAS ® is herein proposed. Different model strategies can be put forward in order to analyze the problem of edge debonding in FRP-strengthened beams. Among them, from the more detailed to the more simplified one, we mention the high-order model, where the behaviour of the RC beam is governed by the classical beam theory, the FRP strip is modelled using the classical lamination theory and the adhesive layer is modelled as a 2D elastic continuum, and the elastic foundation approach with one or two parameters, where the behaviour of the adhesive layer is interpreted as a set of vertical and shear springs connecting the RC beam and the FRP strip. In the finite element method, all the layers can be explicitly modelled or, to simplify the problem as in the present study, a suitable interface constitutive law can be adopted. In this framework, a Mixed-Mode interface constitutive law is considered in order to assess the reliability of using a simplified analytical model accounting only for interface crack sliding and neglecting interface crack opening. A full-range validation of the proposed model is out of the scope of the present work and the reader is referred to (Rabinovitch 2004) for a detailed comparison of the different model strategies.

A 2D model of the retrofitted beam, taking advantage of the symmetry of the problem, is herein considered in the FE discretization. Hence, plane stress eight-noded finite elements are used for the discretization of the continuum. As regards the FRP-concrete bi-material interface, zero-thickness interface elements are used (see Figure 9 for the finite element mesh with partially debonded interface at a given step of the simulation). The mechanical response of these special elements is ruled by a bi-linear cohesive law taking into account the coupling between Mode I and Mode II deformations, as prescribed in CNR-DT 200 2004 (see also Carpinteri *et al*. 2007b,c for similar applications and Paggi *et al*. 2006 for mathematical details). The bi-linear shape of the cohesive law is a simplification of more complex strain-softening relationships (see e.g. Ferretti and Savoia 2003). More specifically, a measure of interface opening and sliding, γ, is introduced:

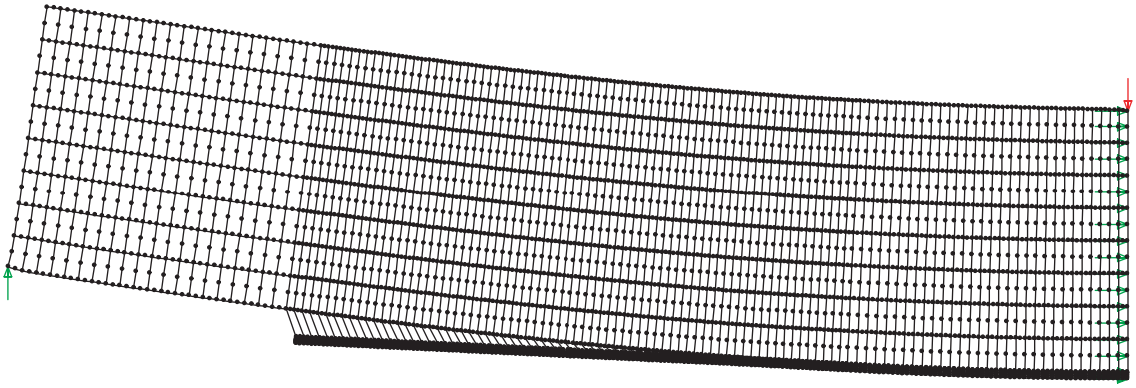

Figure 9. Deformed FE mesh with magnification factor equal to 50 during the edge debonding process

$$\gamma = \sqrt{\left(\frac{g_N}{g_{Nc}}\right)^2 + \left(\frac{g_T}{g_{Tc}}\right)^2} \tag{19}$$

Then, the interface normal and tangential tractions, F_N and F_T, are computed as functions of the opening and sliding displacements:

$$F_N = \begin{cases} \dfrac{\sigma_{max}}{\gamma_{max}} \dfrac{g_N}{g_{Nc}} & \text{for } 0 < \gamma \le \gamma_{max}, \\ \dfrac{\sigma_{max}}{\gamma} \dfrac{1-\gamma}{1-\gamma_{max}} \dfrac{g_N}{g_{Nc}} & \text{for } \gamma_{max} < \gamma < 1; \end{cases}$$

$$F_T = \begin{cases} \dfrac{\tau_{max}}{\gamma_{max}} \dfrac{g_{Nc}}{g_{Tc}} \dfrac{g_T}{g_{Tc}} & \text{for } 0 < \gamma \le \gamma_{max}, \\ \dfrac{\tau_{max}}{\gamma} \dfrac{1-\gamma}{1-\gamma_{max}} \dfrac{g_{Nc}}{g_{Tc}} \dfrac{g_T}{g_{Tc}} & \text{for } \gamma_{max} < \gamma < 1. \end{cases} \tag{20}$$

For either pure normal separation (Mode I), i.e. for $g_T = 0$, or for pure tangential separation (Mode II), i.e. for $g_N = 0$, the classical bilinear cohesive laws are obtained as limit cases. The parameter γ_{max} has not any specific influence on the numerical results, provided that it is chosen sufficiently small as compared to the unity to obtain a very stiff behaviour of the ascending branch of the cohesive law.

The Mode I and Mode II fracture energies are kept equal to 65 N/m, as for the shear-lag model, whereas the maximum shear and normal stresses are estimated according to Eqn 1, i.e. $\tau_{max} = \sigma_{max} = 6.8$MPa. The adopted value of the fracture energy is fully consistent with experimental results in Rabinovitch and Frostig (2003) that present good correlation with the fracture energy values reported by CEB-FIB for concrete (CEB-FIB 1993). To follow the whole mechanical response, the arc-length control-scheme is adopted in order to capture the unstable branch with positive slope (snap-back) after the peak load is achieved. From the physical point of view, this criterion reduces to a crack-length control scheme, i.e. the length of the debonded interface is monotonically increased at each step of the simulation.

As it can be readily seen from Figure 8, an excellent agreement between the analytical prediction and the FE results is achieved, both in terms of critical load and in the shape of the unstable branch, thus proving the soundness of the analytical approach proposed in the present paper. In other words, the Mixed Mode as well as the softening in the cohesive law of the interface affect only slightly the overall structural behaviour of TPB test, since the shear-lag model coupled with a LEFM failure criterion is able to accurately capture the snap-back mechanical response.

Considering now the IC debonding caused by the presence of a flexural crack at mid-span (see Figure 3(a)), it is seen that no snap-through instability occurs since, because of the presence of the flexural crack, the structure is not able to carry any load, if the FRP strip has completely delaminated (we assume the absence of steel bars in the concrete beam). On the other hand, by varying the material parameters (e.g. the FRP stiffness), the slope of the softening branch can change from positive to negative and the snap-back instability at the peak load may disappear. This is clearly shown in Figure 10, where the IC debonding failure of two concrete beams strengthened by FRP plates with different Young's moduli are considered: 140 and 210 GPa respectively (the other mechanical and geometrical properties are the same previously used). The beam with the stiffer FRP is the one showing the highest failure load as well as the snap-back instability at the peak load; in other words, the stronger is the structure, the more brittle is the structural response. Finally observe that, for the geometry with the lower grade reinforcement, the

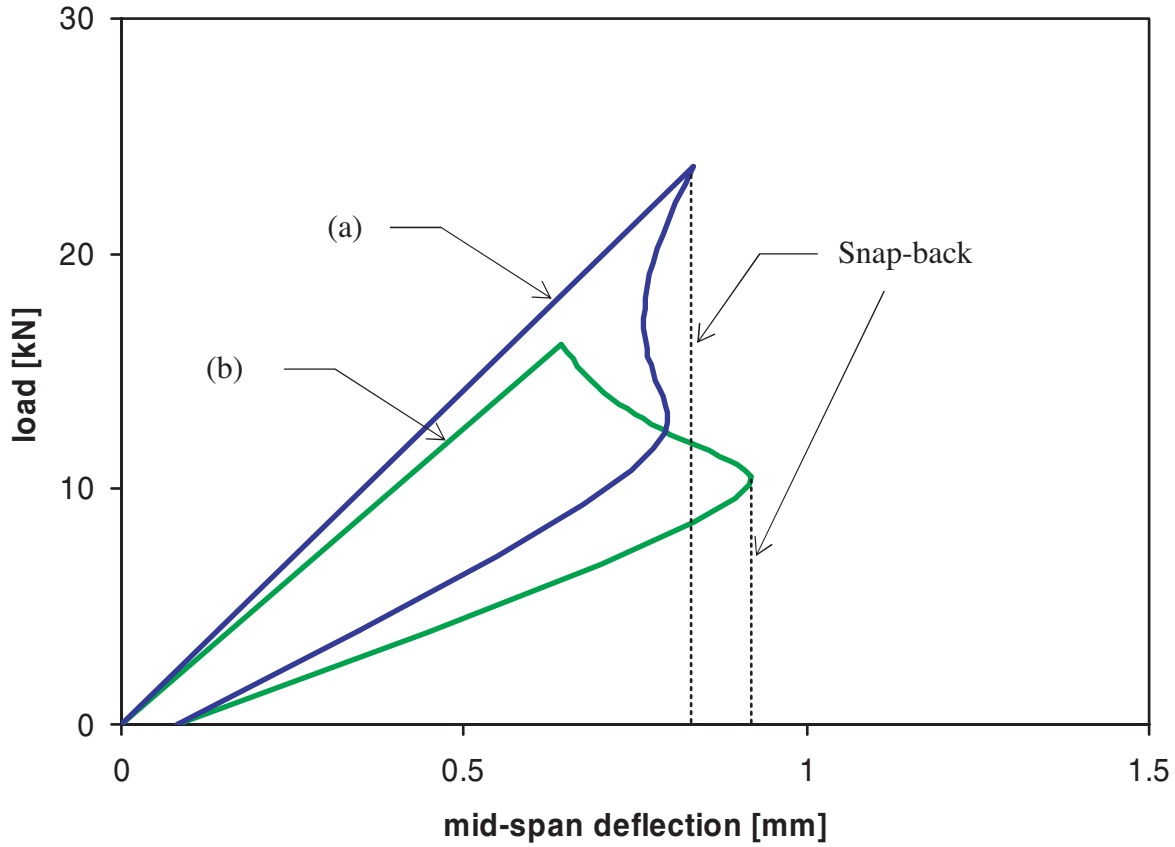

Figure 10. Load vs. mid-span deflection for retrofitted concrete beams undergoing to FRP IC delamination. Curve (a) refers to a beam strengthened by a stiffer FRP with respect to the beam of curve (b)

snap-back instability appears at a later stage in the debonding process.

5. CONCLUSIONS

In the present paper we revisited all the possible failure modes that can occur when dealing with concrete beams strengthened by FRP strips. We focused the attention on the failures due to critical diagonal cracks and to FRP debonding, either from the edge or from an intermediate transversal crack, since these collapses are the ones most commonly observed in engineering practice and laboratory experiments. In particular, we analysed the competition between these failure mechanisms, i.e. critical diagonal crack vs. edge debonding, edge debonding vs. IC debonding, IC debonding vs. flexural crack. The first competition was addressed by analyzing the stress-intensification at the FRP edge, the second competition by a coupled shear lag-LEFM approach and the third one by means of the bridged crack model. Eventually, we highlighted the geometrical and mechanical parameters governing the transition from a failure mode to another.

The present paper showed the basic ideas by which we want to tackle the structural problem under examination. Future developments will include analytical details as well as comparisons with experimental data. Furthermore, once the soundness of the approach were confirmed, we could remove some of the simplifying assumptions we used in the present analysis to achieve a fully analytical formulation.

ACKNOWLEDGEMENTS

The financial support provided by the European Union to the Leonardo da Vinci ILTOF Project (Innovative Learning and Training on Fracture) is gratefully acknowledged.

REFERENCES

Accardi, M. (2004). *Strengthening of Masonry Structural Elements Subjected to Out-of-Plane Loads Using CFRP Reinforcement*, Phd Thesis, Palermo, Italy.

ACI 440R-96 (1996). *State-of-the-Art Report on Fiber Reinforced Plastic (FRP). Reinforcement for Concrete Structures*, American Concrete Institute, Committee 440, Michigan, USA.

Alaee, F. and Karihaloo, B. (2003). "Fracture model for flexural failure of beams retrofitted with CARDIFRC", *Journal of Engineering Mechanics*, ASCE, Vol. 129, No. 9, pp. 1028-1038.

Arduini, M., Di Tommaso, A. and Nanni, A. (1997). "Brittle failure in FRP plate and sheet bonded beams", *ACI Structural Journal*, Vol. 94, No. 44, pp. 363-370.

Ascione, L. and Feo, L. (2000). "Modeling of composite/concrete interface of RC beams strengthened with composite laminates", *Composites Part B: Engineering*, Vol. 31, No 6, pp. 535-540.

Bocca, P., Carpinteri, A. and Valente, S. (1990). "Size effects in the mixed mode crack propagation: softening and snap-back analysis", *Engineering Fracture Mechanics*, Vol. 35, No. 9, pp. 159-170.

Bogy, D. (1971). "Two edge-bonded elastic wedges of different materials and wedge angles under surface tractions", *ASME Journal of Applied Mechanics*, Vol. 38, pp. 377-386.

Carpinteri, A. (1981). "A fracture mechanics model for reinforced concrete collapse", *Proceedings of the IABSE Conference Delft*, pp. 17-30.

Carpinteri, A. (1984). "Stability of fracturing process in R.C. beams", *Journal of Structural Engineering,* ASCE, Vol. 110, No. 3, pp. 544-558.

Carpinteri, A. (1985). "Interpretation of the Griffith instability as a bifurcation of the global equilibrium", In S. Shah (Ed.), Application of Fracture Mechanics to Cementitious Composites, *Proceedings of a NATO Advanced Research Workshop*, Evanston, USA (1984), pp. 287-316. Martinus Nijhoff Publishers, Dordrecht.

Carpinteri, A. (1987). "Stress-singularity and generalized fracture toughness at the vertex of re-entreant corners", *Engineering Fracture Mechanics*, Vol. 26, pp. 143-155.

Carpinteri, A. (1989a). "Cusp catastrophe interpretation of fracture instability", *Journal of the Mechanics and Physics of Solids*, Vol. 37, pp. 567-582.

Carpinteri, A. (1989b). "Decrease of apparent tensile and bending strength with specimen size: two different explanations based on fracture mechanics*", International Journal of Solids and Structures*, Vol. 25, No. 44, pp. 407-429.

Carpinteri, A. and Paggi, M. (2005). "On the asymptotic stress field in angularly nonhomogeneous materials", *International Journal of Fracture*, Vol. 135, No. 1-4, pp. 267-283.

Carpinteri, A. and Paggi, M. (2006). "Influence of the intermediate material on the singular stress field in tri-material junctions", *Materials Science*, Vol. 42, No. 1, pp. 95-101.

Carpinteri, A. and Paggi, M. (2007). "Analytical study of the singularities arising at multi-material interfaces in 2D linear elastic problems", *Engineering Fracture Mechanics*, Vol. 74, No. 1-2, pp. 59-74.

Carpinteri, A., Cornetti, P. and Pugno, P. (2007a). "Debonding in FRP strengthened beams: stress assessment versus fracture mechanics approach", In: *Design, Assessment and Retrofitting of RC Structures*, Vol. 2 of the *Proceedings of the 6th Conference on Fracture Mechanics of Concrete and Concrete Structures* (FraMCoS), Catania, Italy, Taylor & Francis, pp. 1053-1060.

Carpinteri, A., Lacidogna, G. and Paggi, M. (2007b). "Acoustic emission monitoring and numerical modelling of FRP delamination in RC beams with non-rectangular cross-section", *RILEM Materials & Structures*, Vol. 40, pp. 553-566.

Carpinteri, A., Lacidogna, G. and Paggi, M. (2007c). "On the competition between delamination and shear failure in retrofitted concrete beams and related scale effects", In: *Design, Assessment and Retrofitting of RC Structures*, Vol. 2 of the *Proceedings of the 6th Conference on Fracture Mechanics of Concrete and Concrete Structures* (FraMCoS), Catania, Italy, Taylor & Francis, pp. 1069-1076.

CEB-FIB (1993). *Model Code 1990*, London, UK, Thomas Telford.

CNR-DT 200 (2004). "Istruzioni per la Progettazione, l'Esecuzione ed il Controllo di Interventi di Consolidamento Statico mediante l'utilizzo di Compositi Fibrorinforzati. Materiali, strutture di c.a. e di c.a.p., strutture murarie".

Cornetti, P., Puzzi, S. and Carpinteri, A. (2007). "Failure mechanisms in beams strengthened with adesive strips", In *Proceedings of the XVIII AIMETA Conference*, Brescia, Italy.

David, E., Djelal, C. and Buyle-Bodin, F. (1993). "Repair and strengthening of reinforced concrete beams using composite materials", In *Proceedings of the 2nd international PhD symposium in civil engineering*, Budapest.

Ferretti, D. and Savoia, M. (2003). "Cracking evolution in R/C members strengthened by FRP plates", *Engineering Fracture Mechanics*, Vol. 70, pp. 1069-1087.

fib Bulletin (2001). "Design and use of externally bonded FRP reinforcement (FRP EBR) for reinforced concrete structures", *Bulletin No. 14*, prepared by subgroup EBR (Externally Bonded Reinforcement) of fib Task Group 9.3 FRP Reinforcement for Concrete Structures.

Hollaway, L. and Leeming, M. (1999). *Strengthening of Reinforced Concrete Structures*, Cambridge, England: Woodhead Publishing.

JCI (2003). *Technical Report on Retrofitting Technology for Concrete Structures*, Technical Committee on Retrofitting Technology for Concrete Structures.

Leung, C.K.Y. (2001). "Delamination failure in concrete beams retrofitted with a bonded plate", *Journal of Materials in Civil Engineering*, ASCE, Vol. 13, No. 2, pp. 106-113.

Leung, C. (2004), "Fracture mechanics of debonding failure in FRP-strengthened concrete beams", In V. Li, C. Leung, K. Willam, and S. Billington (Eds.), *Proceedings of the 5th International Conference on Fracture Mechanics of Concrete and Concrete Structures (FraMCoS-5)*, Vail, Colorado, USA, Vol. 1, pp. 41-52.

Leung, C.K.Y. and Yang, Y. (2006). "Energy-based modeling approach for debonding of FRP plate from concrete substrate", *Journal of Engineering Mechanics*, ASCE, Vol. 132, pp. 583-593.

Maalej, M. and Leong, K. (2005). "Effect of beam size and FRP thickness on interfacial shear stress concentration and failure mode of FRP strengthened beams", *Composites Science and Technology*, Vol. 65, No. 7-8, pp. 1148-1158.

Malek, A., Saadatmanesh, H. and Ehsani, M. (1998). "Prediction of failure load of R/C beams strengthened with FRP plate due to stress concentration at the plate end", *ACI Structural Journal*, Vol. 95, No. 1, pp. 142-152.

Muckopadhyaya, P. and Swamy, N. (2001). "Interface shear stress: a new design criterion for plate debonding", *Journal of Composite Construction*, Vol. 5, pp. 35-43.

Oehlers, D.J. and Seracino, R. (2004). *Design of FRP and Steel Plated RC Structures: Retrofitting Beams and Slabs for Strength , Stiffness and Ductility*, Amsterdam : Elsevier.

Paggi, M., Carpinteri, A. and Zavarise, G. (2006). "A unified interface constitutive law for the study of fracture and contact problems in heterogeneous materials", In: P. Wriggers, U. Nackenhorst (Eds.), *Analysis and Simulation of Contact Problems, Lecture Notes in Applied and Computational Mechanics*, Vol. 27, pp. 297-304, Springer-Verlag, Berlin.

Qian, Z. and Akisanya, A. (1999). "An investigation of the stress singularity near the free edge of scarf joints", *European Journal of Mechanics A/Solids*, Vol. 18, pp. 443-463.

Rabinovitch, O. (2004). "Fracture-mechanics failure criteria for RC beams strengthened with FRP strips-A simplified approach", *Composite Structures*, Vol. 64, No. 3-4, pp. 479-492.

Rabinovitch, O. and Frostig, Y. (2001). "Delamination failure of RC beams strengthened with FRP strips-A closed form high-order and fracture mechanics approach", *Journal of Engineering Mechanics,* ASCE, Vol. 127, No. 8, pp. 852-861.

Rabinovitch, O. and Frostig, Y. (2003) "Experiments and analytical comparison of RC beams strengthened with CFRP strips", *Composites Part B: Engineering*, Vol. 34, pp. 663-677.

Reedy, J. and Guess, T. (1993). "Comparison of butt tensile strength data with interface corner stress intensity factor prediction", *International Journal of Solids and Structures*, Vol. 30, pp. 2929-2936.

Smith, S.T. and Teng, J.G. (2001). "Interfacial stresses in plated beams", *Engineering Structures*, Vol. 23, No. 7, pp. 857-871.

Smith, S.T. and Teng, J.G. (2002a). "FRP-strengthened RC beams. I: review of debonding strength models", *Engineering Structures*, Vol. 24, No. 4, pp. 385-395.

Smith, S.T. and Teng, J.G. (2002b). "FRP-strengthened RC beams. II: assessment of debonding strength models", *Engineering Structures*, Vol. 24, No. 4, pp. 397-417.

Stang, H., Li, Z. and Shah, S.P. (1990). "Pullout problem: stress versus fracture mechanical approach", *Journal of Engineering Mechanics*, ASCE, Vol. 116, pp. 2136-2150.

Taljsten, B. (1997). "Strengthening of beams by plate bonding", *Journal of Materials in Civil Engineering*, ASCE, Vol. 9, No. 4, pp. 206-212.

Teng, J.G., Smith, S.T., Yao, J. and Chen, J.F. (2003). "Intermediate crack-induced debonding in RC beams and slabs", *Construction and Building Materials*, Vol. 17, No. 6-7, pp. 447-462.

Wang, J. (2006). "Cohesive zone model of intermediate crack-induced debonding of FRP-plated concrete beam", *International Journal of Solids and Structures*, Vol. 43, No. 21, pp. 6630-6648.

Williams, M. (1952). "Stress singularities resulting from various boundary conditions in angular corners of plates in extension", *ASME Journal of Applied Mechanics*, Vol. 74, pp. 526-528.